ELSEVIER

Contents lists available at ScienceDirect

Chemical Engineering Journal

journal homepage: www.elsevier.com/locate/cej





Bio-based, selenium/Schiff base-containing co-curing agent enables flame-retardant, smoke-suppressive and mechanically-strong epoxy resins

Qian Zhong ^a, Cheng Wang ^{a,*}, Guofeng Ye ^a, Zhenghong Guo ^b, Ting Sai ^b, Min Hong ^c, Pingan Song ^c, Hao Wang ^d, Siqi Huo ^{d,*}, Zhitian Liu ^{a,*}

- ^a Hubei Engineering Technology Research Center of Optoelectronic and New Energy Materials, Hubei Key Laboratory of Plasma Chemistry and Advanced Materials, School of Materials Science & Engineering, Wuhan Institute of Technology, Wuhan, 430205, China
- b Institute of Fire Safety Materials, School of Materials Science and Technology, NingboTech University, Ningbo, 315100, China
- ^c School of Engineering, Centre for Future Materials, University of Southern Queensland, Springfield Central, 4300, Australia
- d School of Agriculture and Environmental Science, Centre for Future Materials, University of Southern Queensland, Springfield Central, 4300, Australia

ARTICLE INFO

Keywords: Epoxy resin Organoselenium Schiff base Flame retardancy Mechanical strength

ABSTRACT

Epoxy resins (EPs) have excellent overall properties, but their inherent flammability severely limits their industrial applications. Most existing flame-retardant methods rely on phosphorus-based compounds. However, they suffer from bioaccumulation and potential risks to ecosystems and human health. The development of safer and more sustainable phosphorus-free flame-retardant EP systems based on biomass is highly promising but challenging. Herein, a selenium/Schiff base-containing, bio-based flame retardant (SNC) has been successfully synthesized and applied as a multifunctional co-curing agent in EP. The resultant EP containing 15 wt% SNC (EP-SNC15) exhibits enhanced mechanical strength. Additionally, EP-SNC15 achieves a high limiting oxygen index (LOI) of 31.8 % and a vertical burning (UL-94) V-0 rating, and its peak heat release rate (PHRR) and total heat release (THR) decrease by 73.3 % and 56.3 % compared to EP, respectively. Therefore, the excellent flame retardancy and mechanical properties of EP-SNC15 make it superior to previously reported phosphorus-free flame-retardant epoxy systems. The improvement in flame retardancy is attributed to the synergistic catalytic carbonization of selenium-containing and Schiff base groups in SNC in the condensed phase and the free radical quenching of organoselenium groups in the gas phase. Therefore, this work provides a novel design strategy for the development of next-generation, flame-retardant and bio-based EPs.

1. Introduction

EP is a commonly used thermosetting resin, valued in construction, transportation, and aviation for its excellent bonding strength, electrical insulation, and thermal stability. However, in common with most petroleum-based polymers, its inherent flammability leads to the generation of excessive heat and dense smoke particles during combustion, posing serious challenges to evacuation and firefighting efforts [1-5]. Hence, reducing flammability and improving smoke suppression are key challenges in flame-retardant polymer research.

To address this issue, many strategies have been adopted with remarkable results. Incorporating flame retardants has proven to be a simple and effective solution [6]. Traditional halogen-based flame retardants are inexpensive and effective, but they release toxic and corrosive gases during combustion, posing serious threats to human health

and the environment [7]. Thus, many of these halogen-based flame retardants have been strictly regulated or banned. Phosphorus-based flame retardants, due to their halogen-free, low toxicity, and significant flame-retardant effects in both the gas and condensed phases, are considered the most promising alternatives to halogen-based flame retardants. Based on their application methods, they can be classified into additive-type and reactive-type flame retardants. Compared with additive-type phosphorus flame retardants, reactive flame retardants exhibit superior compatibility with the EP matrix and long-lasting, efficient flame-retardant performance, as their flame-retardant groups are covalently bonded to the EP backbone through chemical modification. Wang et al. [8] synthesized a phosphorus-containing epoxy curing agent (ADIM). Benefiting from the radical quenching effect and catalytic charring ability of ADIM, the EP/ADIM composites exhibited excellent flame retardancy, achieving an LOI of 35.0 % and a UL-94 V-0 rating.

E-mail addresses: cheng.wang@wit.edu.cn (C. Wang), Siqi.Huo@unisq.edu.au, sqhuo@hotmail.com (S. Huo), able.ztliu@wit.edu.cn (Z. Liu).

^{*} Corresponding authors.

Chen et al. [9] developed a co-curing agent containing phosphorus, nitrogen, and boron (TMDB), which was used to construct intrinsically flame-retardant epoxy systems. Upon incorporation of 15.1 wt% TMDB, the resulting EP composite reached a UL-94 V-0 rating and an LOI value of 29.6 %. Liu et al. [10] developed an hyperbranched polyborophosphate/epoxy resin (HPBP/EP) material. This dual dynamic B-O and P-O linkage structure exhibits excellent flame-retardant properties, enabling the material to achieve a maximum oxygen index of 33 % and an UL-94 V-0 rating. Although reactive phosphorus-based flame retardants have been widely used to improve the flame retardancy of epoxy resins and have demonstrated excellent comprehensive performance, their potential bioaccumulation and aquatic toxicity have raised growing environmental and health concerns. Therefore, the development of halogen- and phosphorus-free reactive flame-retardant systems has emerged as a critical direction toward achieving green chemistry and sustainable materials.

In the field of flame-retardant thermosetting resins, the advancement of phosphorus-free strategies has been primarily driven by the synergistic effects of alternative flame-retardant elements (such as silicon, nitrogen, boron, and sulfur) and the ongoing exploration of molecular flame retardants with unique structural features. Zhang et al. [11] reported a phosphorus-free hyperbranched polyborate (HBPB) as a multifunctional flame-retardant additive for EP. Compared with EP, the EP composite containing 9 wt% HBPB exhibited enhanced fire resistance, achieving an LOI of 30.2 % and a UL-94 V-0 rating. It significantly reduced fire hazards such as smoke production, heat release, and toxic gas emission without the introduction of phosphorus-based components. Niu et al. [12] synthesized a Schiff base-containing epoxy monomer (triazole-va-EP), which was subsequently cured with 4,4 '-diaminodiphenylmethane (DDM) to obtain a bio-based EP. The LOI value of this EP was 39.5 %, and the UL-94 rating reached V-0. Selenium, a naturally occurring non-metallic trace element, shares similar chemical properties with sulfur, yet exhibits stronger electron cloud polarizability and higher reactivity toward free radicals. Compared with inorganic selenium compounds (e.g., SeO2), which pose concerns related to toxicity and bioaccumulation, organoselenium compounds have garnered increasing attention in life sciences and materials research due to their tunable molecular structures, lower toxicity, and excellent thermal stability. It is worth noting that Se-containing organic compounds can effectively quench oxygen-centered radicals (e.g., ·OH and ·O), thereby slowing down the thermal degradation process and suppressing flame propagation [13]. Compared with Si- and B-based flame retardants that mainly function through condensed-phase barrier formation, seleniumcontaining systems provide dual-phase protection. Organoselenium compounds can efficiently quench oxygen-centered radicals in the gas phase while catalyzing carbonization in the condensed phase, thereby achieving simultaneous suppression of heat release and smoke generation. Therefore, the use of organoselenium groups to design phosphorusfree flame retardants with dual flame retardant effects is an effective yet challenging strategy for the development of high-performance, environmentally friendly EPs.

In addition, bio-based materials have the characteristics of being environmentally friendly and low in cost [14,15]. The design and preparation of green flame retardants with novel molecular structures using biomass such as phytic acid [16,17], vanillin [18,19], chitosan [20–22], itaconic acid [23], cinnamic acid [24], and lignin [25,26] is also a current research hotspot in the discipline of flame retardant polymers. For instance, Tang et al. [27] developed a bio-based flame retardant (V-Cc-PP) from vanillin and phytic acid (PA) and applied it to EP. The addition of 4.0 wt% V-Cc-PP reduced the PHRR by 34.2 %. Yu et al. [28] synthesized a novel bio-based intumescent flame retardant (TLI) to prepare EP/TLI intumescent coatings. When the amount of TLI was 20 wt%, the LOI and UL-94 rating of EP/TLI were 26.5 % and V-0. Salicylic acid is a naturally occurring organic acid, which is abundantly in various plants, including willow bark and wintergreen leaves. Due to the presence of reactive functional groups, salicylic acid can be used as a

raw material to synthesize various compounds with tunable functionalities.

In this work, a selenium/Schiff base-containing bio-based flame retardant (SNC) was prepared using 3, 4-diaminotoluene, selenium dioxide and 5-aminosalicylic acid, which was applied in EPs as a co-curing agent. The influence of SNC on the thermal stability, mechanical properties, flame retardancy and smoke suppression of EP were systematically investigated, and the mechanisms of reinforcement and flame retardancy were deeply elucidated. This work provides an effective approach for the design of phosphorus-free, bio-based flame retardants, with promising potential for widespread application in thermosetting resins.

2. Material and methods

2.1. Materials

Diglycidyl ether of bisphenol-A (DGEBA, CYD-127, epoxide equivalent weight: ~185 g/equiv) was provided by Yueyang Baling Petrochemical Co., Ltd. (Hunan, China). 3,4-diaminotoluene, 5-aminosalicylic acid (5-ASA) and 4,4 '-diamino-diphenylmethane (DDM) were purchased from Energy Chemical Co., Ltd. (Shanghai, China). Selenium dioxide was supplied by Macklin Biochemical Technology Co., Ltd. (Shanghai, China). Xylene and absolute ethanol were provided by Sinopharm Chemical Reagent Co., Ltd. (Shanghai, China).

2.2. Synthesis of Se-derived intermediate (S-2 N)

The schematic diagram of the synthetic route for SNC is shown in Fig. 1a. 3,4-diaminotoluene (2.0 g, 16.37 mmol) and selenium dioxide (4.54 g, 40.93 mmol) were dissolved in 50 mL of xylene, then condensed and refluxed for 24 h. The reaction mixture was filtered while hot to obtain the liquid phase, and xylene was removed by rotary distillation at 125 °C. The resulting brown solid product, S-2N, was dried in a vacuum oven at 120 °C overnight.

2.3. Synthesis of flame retardants containing Se (SNC)

5-Aminosalicylic acid (2.00 g, 13.06 mmol) and S-2N (2.7 g, 12.80 mmol) were added to a flask with 50 mL of anhydrous ethanol as the solvent. The mixture was stirred under a nitrogen atmosphere at 80 $^{\circ}\text{C}$ for 6 h. After the reaction, the mixture was filtered while hot, and the solid product was washed 2–3 times with anhydrous ethanol and vacuum-dried at 80 $^{\circ}\text{C}$ overnight to yield the final product (SNC).

2.4. Preparation of EP samples

The proportions of each component in the EP samples are listed in Table S1. The preparation procedure is as follows: the epoxy resin and SNC were mixed thoroughly by mechanical stirring at 50 $^{\circ}$ C, after which DDM was added and stirred rapidly for 7 min. The mixture was then degassed under vacuum for 3 min and poured into a preheated mold at 80 $^{\circ}$ C. The curing process was carried out in stages: 80 $^{\circ}$ C for 0.5 h, 100 $^{\circ}$ C for 2 h, 120 $^{\circ}$ C for 2 h, and finally 150 $^{\circ}$ C for 4 h. Based on the SNC content (5, 10, and 15 wt%), the samples were designated as EP-SNC5, EP-SNC10, and EP-SNC15, respectively. For comparison, the EP sample was prepared using the same method without the addition of SNC.

2.5. Characterizations

This is provided in the Supporting information.



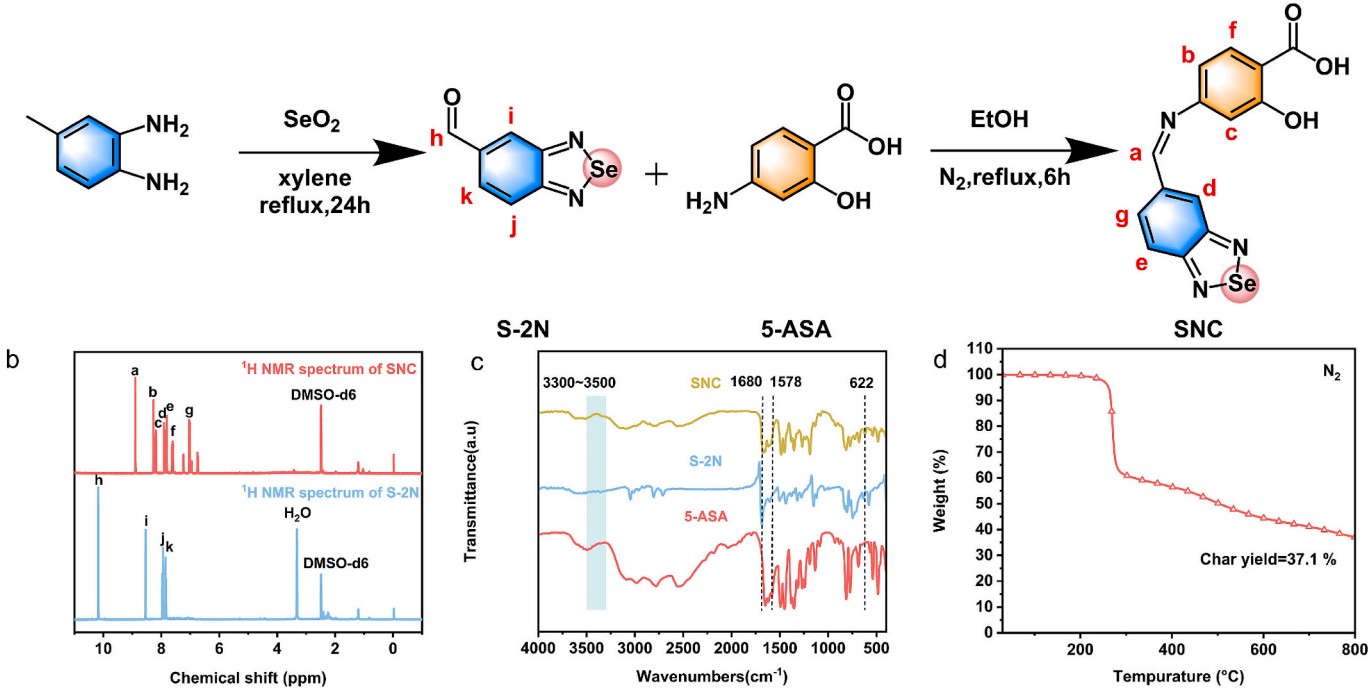


Fig. 1. (a) Schematic diagram of SNC synthesis; (b) 1H NMR spectra of S-2 N and SNC; (c) FTIR spectra of 5-ASA, S-2 N, and SNC; and (d) TG curve of SNC.

3. Results and discussion

3.1. Preparation and characterization of SNC

The schematic diagram of SNC synthesis is shown in Fig. 1a. The chemical structure characterization of SNC was carried out by $^1\mathrm{H}$

nuclear magnetic resonance (NMR) and Fourier transform infrared spectroscopy (FTIR). In Fig. 1b, the aldehyde proton signal appeared at 10.17 ppm for S-2N. After the reaction of S-2N with 5-aminosalicylic acid, the aldehyde proton signal at 10.17 ppm disappeared, followed by the appearance of the -CH=N- signal at 8.9 ppm, indicating the successful synthesis of SNC [6,29]. As shown in Fig. 1c, the FTIR spectra

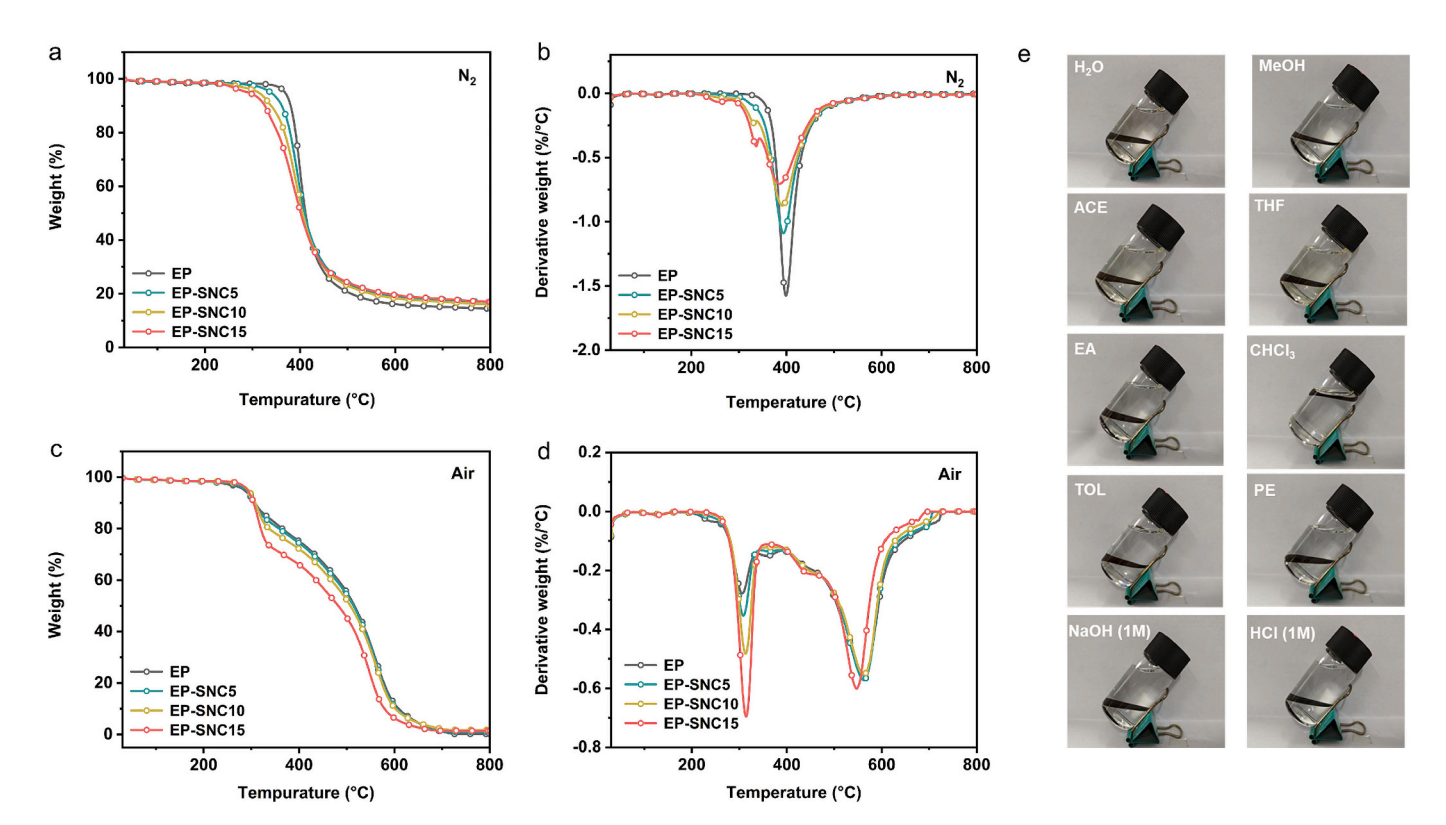


Fig. 2. (a) TG curves and (b) DTG curves of EP samples under N₂ atmosphere; (c) TG curves and (b) DTG curves of EP samples under air atmosphere; (e) Digital photos of EP-SNC samples after being immersed in different solvents for 240 h.

reveal that 5-ASA, S-2N, and SNC exhibit an -OH absorption band in the range of 3300-3500 cm⁻¹ [30]. 5-ASA displays an N-H stretching vibration peak at 1578 cm⁻¹ [31], which disappears in the FTIR spectrum of SNC, indicating that the N-H groups have been fully reacted. In addition, SNC shows characteristic peaks at 1680 and 622 cm⁻¹, corresponding to C=N and Se-N bonds, respectively, further confirming the successful synthesis of SNC [32,33]. Additionally, thermogravimetric analysis (TGA) was conducted to study the thermal stability of SNC under nitrogen and air conditions, with the relevant curves and characteristic data shown in Fig. 1d, S1 and Table S2. SNC exhibits initial decomposition temperature ($T_{5\%}$, temperature at 5 wt% weight loss) values of 262 $^{\circ}\text{C}$ in air and 261 $^{\circ}\text{C}$ in nitrogen, both of which are higher than the curing reaction temperature of the EP-SNC samples, indicating that SNC maintains good thermal stability during curing and does not undergo premature degradation. Meanwhile, the char yields at 800 °C of SNC are 0.2 % in air and 37.1 % in nitrogen, suggesting that it possesses a great char-forming capability.

3.2. Thermal stability and solvent resistance of EP-SNC

The thermal stability of EP and EP-SNC samples was studied by thermogravimetric analysis under N₂ and air atmospheres. The relevant data are shown in Fig. 2a-d and Table S2. As shown in Fig. 2a and b, all EP samples exhibit the same degradation trend under N2 and air atmospheres. Under N2 atmosphere, both EP and EP-SNC are degraded in one stage within the range of 300 to 500 °C, which is due to the decomposition of the polymer framework [34]. The incorporation of SNC leads to a decrease in the $T_{5\%}$ of the EP samples, which may be attributed to the catalytic effect of the organoselenium component, promoting early degradation of the polymer matrix [13]. Further, the EP-SNC samples exhibit a stronger charring capacity than EP because of the introduction of organoselenium group (see Table S2). For example, EP-SNC15 shows a char yield of 16.9 %, which is 16.6 % higher than that of EP (14.5 %). Such enhanced char formation ability indicates the flame-retardant effect of EP-SNC in the condensed phase to a certain extent. In addition, the degradation of EP and EP-SNC includes two stages under an air atmosphere (see Fig. 2c and d). The first stage is mainly the thermal decomposition of polymer backbone, and the second stage is the thermal oxidation decomposition of residual char [7]. The $T_{5\%}$ of the EP-SNC sample is significantly increased, indicating that organic selenium can improve the thermal stability in air atmosphere [13]. Furthermore, the char yield of the EP-SNC samples is higher than that of EP and they are increased with the increase of SNC content, further confirming the promoting carbonization effect of organic selenium.

Since SNC is introduced into the epoxy resin system as a co-curing agent, the selenodiazole groups contained in its structure can provide strong intermolecular forces and are prone to form a cross-linked network structure. However, this structure is susceptible to the influence of solvents [35]. The solvent resistance experiment was conducted on the EP-SNC15 spline, and the results are shown in Fig. 2e. This spline can effectively maintain its structural integrity for more than 240 h in various polar and non-polar solvents such as water, methanol (MeOH), acetone (ACE), tetrahydrofuran (THF), ethyl acetate (EA), chloroform (CHCl₃), toluene (TOL), petroleum ether (PE), 1 M NaOH solution and 1 M HCl solution. This indicates that EP-SNC15 exhibits good solvent resistance.

3.3. Mechanical properties of EP-SNC

The curing behavior of EP and EP-SNC15 systems were systematically analyzed via differential scanning calorimetry (DSC), and the relevant data showed in Fig. S2 and Table S3. Both mixtures exhibit a single curing exothermic peak. And the peak curing temperature (T_p) of EP-SNC15 is significantly lower than that of EP, which may be attributed to the early ring opening of the epoxy groups catalyzed by the phenolic hydroxyl and carboxyl groups in SNC. Moreover, the Kissinger, Crane,

and Flynn-Wall-Ozawa (FWO) methods were employed to investigate the curing kinetics, and the corresponding linear fittings of $\ln(\beta/T_p^2)$ vs. $1/T_p$ and $\ln(\beta)$ vs. $1/T_p$ are presented in Fig. S2c and d. The reaction model was first established using the Kissinger method and further validated by the FWO approach. The calculated kinetic parameters and the obtained E_a are listed Table S3. The E_a is a commonly used indicator for evaluating the curing activity of resins. Compared to EP, EP-SNC15 sample exhibit higher E_a values. This mainly originates from the fact that SNC acts as a co-curing agent to consume part of the epoxy groups, which reduces the effective reaction site of the epoxy-amine curing reaction and introduces a spatial site resistance, thus increasing the energy barrier of the curing reaction.

The mechanical properties of EP and EP-SNC samples were studied, with detailed results presented in Fig. 3, S3 and Table S4, S5. The storage modulus (E') and tan δ plots were obtained by dynamic mechanical analysis (DMA), and the results are shown in Fig. 3a-c and Table S4. According to the classical theory of rubber elasticity, the crosslinking density (v) is calculated according to the formula: v = E/3RT, where R is the gas constant and E is the E' corresponding to the temperature being 30 °C higher than T_g [36,37]. Due to the introduction of SNC, the glass transition temperature (T_g) of EP-SNC samples decreases, mainly because of the decrease in v (see Fig. 3c and Table S4). During the curing process, the carboxyl and phenolic hydroxyl groups in SNC react with the epoxy groups of EP, resulting in covalent bonding between SNC and the EP/DDM cross-linked network. This may interfere with the complete curing of the epoxy system, thereby reducing the v. Moreover, the static mechanical property test results of EP and EP-SNC samples are shown in Fig. 3d-f and Table S5. The addition of SNC can effectively enhance the mechanical performance of EP-SNC samples. In detail, the tensile strength and Young's modulus (75.3 MPa and 2792.3 MPa) of EP-SNC15 are higher than those of EP (50.9 MPa and 1302.4 MPa). The impact strength and toughness of EP-SNC15 are 3.2 kJ/m² and 1.44 MJ/m³, which are slightly higher than those of pure EP (3.1 kJ/m² and 1.41 MJ/ m³), further demonstrating enhanced mechanical strength and toughness. The improvement in mechanical performance is attributable to the increased spatial site resistance of the rigid benzene structure and the supramolecular bonding interactions formed between the selenadiazole structure in SNC [35]. Such reinforcement and toughening effects have also been reported in previous studies [7].

To evaluate the action mechanism of SNC, the fracture surfaces of EP and EP-SNC samples after Izod impact testing were examined by scanning electron microscopy (SEM) and energy dispersive X-ray spectrometry (EDS) techniques, with the results shown in Fig. S3. The cross-section of the EP sample is smooth, reflecting the characteristics of brittle fracture. The fracture surfaces of EP/SNC10 and EP/SNC15 become rougher, with numerous folds and crack structures (Fig. S3b and c), which significantly increase the fracture area and lengthen the crack extension paths, thus effectively dissipating more fracture energy and improving the impact toughness of the materials. The Se-element mapping on the surface of EP/SNC10 and EP/SNC15 samples reveals that SNC acts as a co-curing agent to form covalent bonds with the cross-linked network of EP, which is uniformly distributed inside the matrix, thus enhancing the mechanical properties of the samples.

3.4. Flame-retardant performance of EP-SNC

The fire safety of EP and EP-SNC samples was tested by LOI, UL-94 and cone calorimeter test (CCT), with the specific test results shown in Fig. 4 and Table S6–7. The LOI values and UL-94 rating of the samples are listed in Table S6. The LOI value of EP is 26.8 % and it fails the UL-94 rating, indicating that EP is a highly flammable material [38]. With the introduction of SNC, the LOI value and UL-94 rating of EP-SNC significantly increase. Meanwhile, the flame retardant properties are gradually enhanced with the increase of SNC addition. In detail, when the addition amount of SNC is 15 wt%, EP-SNC15 exhibits an LOI value of 31.8 % and passes a UL-94 V-0 rating, thus it is a self-extinguishing material. The

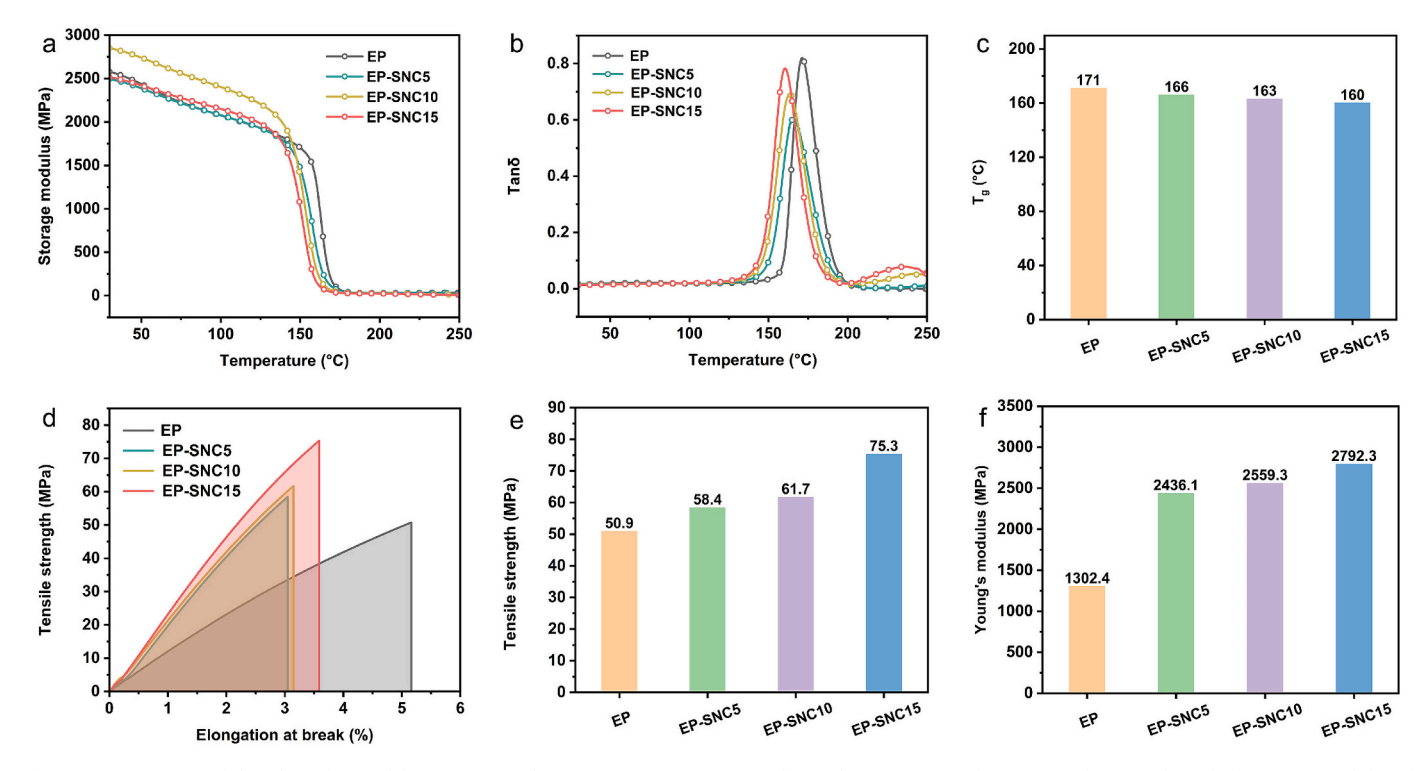


Fig. 3. (a) Storage modulus plots, (b) tan delta curves, (c) glass transition temperature, (d) tensile stress-strain plots, (e) tensile strength, and (f) Young's modulus of the EP samples.

results show that the introduction of SNC can significantly improve the flame retardancy of EP-SNC samples.

To quantitatively characterize the flame retardancy of EP samples, CCT was performed on EP samples. The results are shown in Fig. 4 and Table S7. The PHRR and THR of the EP sample are 1326.2 kW/m² and 77.8 MJ/m², respectively. The PHRR and THR of EP-SNC samples are greatly lower than those of EP. For instance, the PHRR and THR of EP-SNC15 are 354 kW/m² and 33.9 MJ/m², respectively, with 73.3 % and 56.3 % decreases compared with those of EP (see Fig. 4a and b). Therefore, SNC can effectively inhibit the heat release of EP during the combustion process. The fire growth rate (FIGRA) and fire performance index (FPI) are used to evaluate the fire safety of materials, with specific values are shown in Fig. 4c and f. A higher FPI and a lower FIGRA indicate improved fire safety performance of the material [39]. The FPI of EP-SNC15 (0.17 m² s/kW) is significantly higher than that of EP $(0.06 \text{ m}^2 \cdot \text{s/kW})$, while its FIGRA $(8.3 \text{ kW/m}^2/\text{s})$ is markedly lower than that of EP (2.4 kW/m²/s), indicating a substantial enhancement in fire safety performance.

EP materials usually release a large amount of smoke when burning, which seriously affects their application [40]. The peak smoke production rate (PSPR) and total smoke production (TSP) of EP are up to 0.32 m²/s and 28.4 m², respectively, indicating considerable smoke toxicity, which poses significant challenges for fire evacuation and suppression (see Fig. 4e, S4 and Table S7). In contrast, the incorporation of SNC endows the EP samples with improved smoke suppression performance, as evidenced by reduced PSPR and TSP values. Specifically, the PSPR of EP-SNC5 decreases by 25.0 % compared to that of neat EP, while the TSP of EP-SNC15 reduces by 19.4 %. These results demonstrate that the incorporation of SNC effectively suppresses smoke generation and contributes to enhanced fire safety of the material. The average effective heat of combustion (AEHC) and residual char (RC) after combustion for the EP and EP/SNC samples are presented in Fig. 4d, g, and Table S7. The AEHC is an important parameter for evaluating the combustion degree of gaseous volatile substances [41]. The AEHC of EP-SNC samples decreases significantly with increasing SNC content. At a SNC addition of 15 wt%, the AEHC reduces from 22.9 MJ/kg of neat EP to

12.0 MJ/kg, exhibiting a decrease of 47.6 %. Such a change is mainly attributed to the free radical quenching effect of the active fragments derived from SNC, inhibiting the complete progress of the combustion reaction. In addition, the RC values of EP-SNC thermosets are all higher than that of EP, which is consistent with the results of thermogravimetric analysis, further demonstrating the catalytic carbonization of SNC.

According to previous studies [42], the flame-retardant mechanisms of flame retardants primarily involve three pathways: flame inhibition in the gas phase (FIE), and barrier protection (BPE) as well as catalytic char formation (CE) in the condensed phase. All EP-SNC samples exhibit higher FIE, BPE and CE values, indicating their combined gas-phase flame inhibition and condensed-phase barrier/protective effects during combustion (see Fig. 4h, i and S5). With increasing SNC content, both FIE and CE values increase concurrently, further confirming the progressive enhancement of radical scavenging in the gas phase and catalytic char formation in the condensed phase. Therefore, SNC acts synergistically in both the gas and condensed phases to suppress heat release and smoke generation effectively, thereby significantly improving the overall flame-retardant performance of EP.

3.5. Property comparison

The comprehensive performance of EP-SNC samples is compared with that of unmodified EP and previously reported phosphorus-free flame-retardant epoxy systems (Fig. 5 and Table S8) [11,43–51]. The results indicate that the chemically incorporation of Se/Schiff base-containing groups into the cross-linked network significantly enhances the flame retardancy, smoke suppression, and mechanical properties of the EP-SNC system (Fig. 5a). Notably, EP-SNC15 exhibits a higher LOI value than neat EP, and its PHRR and THR reductions are more obvious than those of most phosphorus-free flame-retardant EPs reported in previous works, which can be attributed to the radical-scavenging effect of Se groups in the gas phase and catalytic charring function of Secontaining and Schiff base groups in the condensed phase (Fig. 5b). In addition, the rigid benzene rings and noncovalent interactions

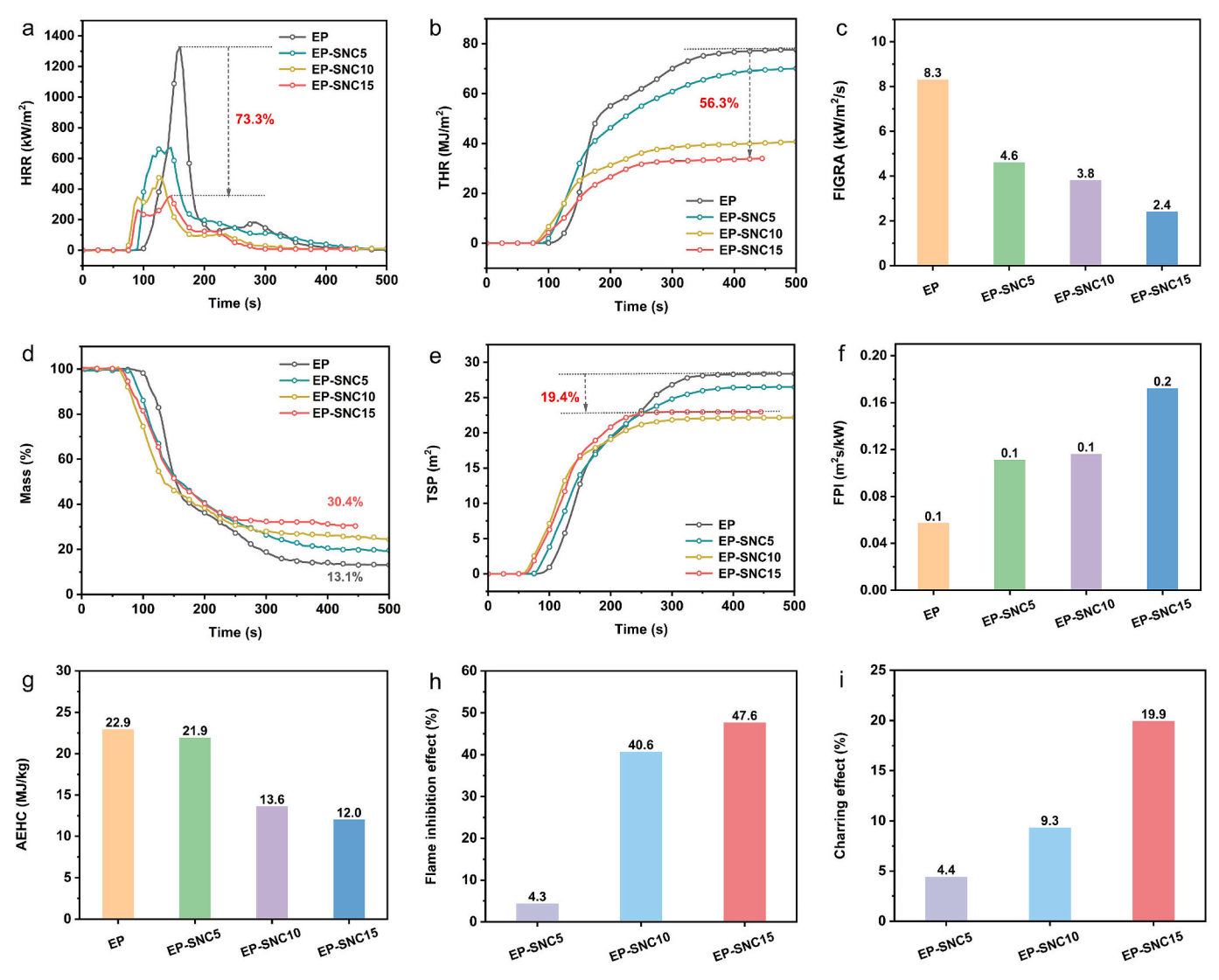


Fig. 4. (a) Heat release rate curves, (b) total heat release curve, (c) fire growth rate (FIGRA), (d) mass loss, (e) total smoke production curves, (f) fire performance index (FPI), (g) average effective heat of combustion (AEHC), (h) flame inhibition effect, (i) charring effect of EP samples.

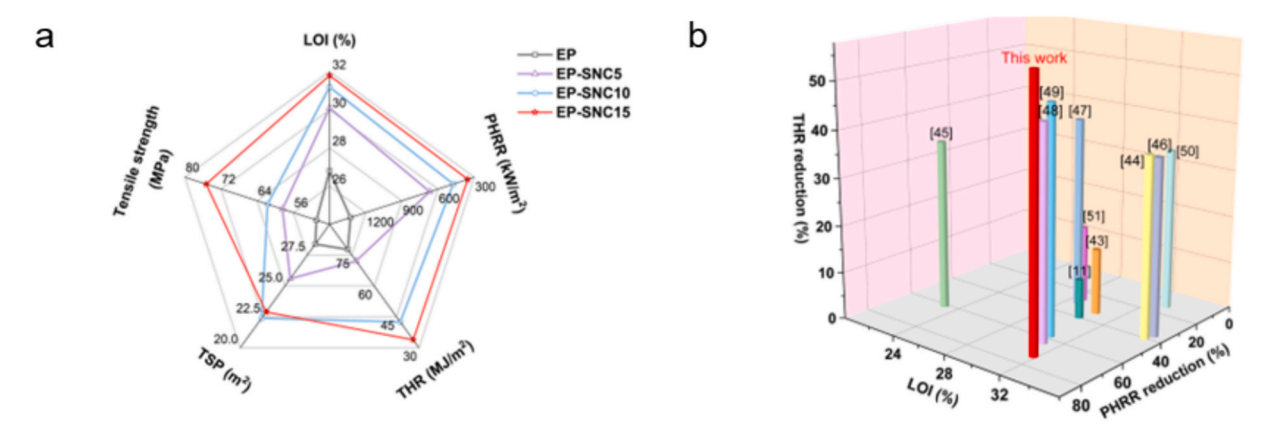


Fig. 5. (a) Property comparison of the flame-retardant properties and mechanical properties of EP with different SNC contents; and (b) the LOI and PHRR and THR reductions of the previously reported phosphorus-free flame-retardant epoxy systems and EP-SNC15.

associated with Se-containing groups in SNC contributed to improved mechanical properties, resulting in superior strength compared to other phosphorus-free flame-retardant system. In summary, the EP-SNC15 sample demonstrates outstanding overall performance in terms of flame retardancy, smoke suppression, and mechanical strength, highlighting the great potential of Se-containing flame retardants for the development of high-performance phosphorus-free flame-retardant epoxy systems.

3.6. Flame-retardant action of SNC

3.6.1. Condensed phase

To investigate the condensed-phase flame-retardant mechanism of SNC, the macro- and micro-morphologies of the char residues after cone calorimetry tests were examined using a digital camera and SEM (see Fig. S6). After combustion, the neat EP sample shows only a small amount of fragmented char with a thickness of approximately 10 mm (Fig. S6a and b). Meanwhile, the EP char surface exhibits numerous cracks and pores, indicating poor flame-retardant and smoke-suppression performance. In contrast, the EP-SNC10 and EP-SNC15 samples form denser and more intumescent char layers, and the thickness of EP-SNC15 char is up to 23 mm, representing an increase of approximately 130 %. This enhancement effect may be attributed to the synergistic catalytic charring function of selenium-containing and Schiff base groups in SNC, which helps to inhibit heat transfer and smoke emission, thereby significantly enhancing flame-retardant and smoke-suppression performance.

To further explore the action mode of SNC in the condensed phase, Raman spectroscopy and X-ray photoelectron spectroscopy (XPS) were employed. The relevant results are shown in Fig. 6 and Table S9. In Fig. 6a, the D peak and G peak of the residual char at $1354~{\rm cm}^{-1}$ and $1586~{\rm cm}^{-1}$ belong to the vibrations of amorphous C atoms and

graphitized C atoms, respectively. The area ratio of peak D to peak G ($I_{\rm D}/I_{\rm G}$) is negatively correlated with the graphitization degree of the char layer [52,53]. The $I_{\rm D}/I_{\rm G}$ value of EP-SNC15 (2.78) is significantly lower than that of pure EP (3.07), indicating a higher degree of graphitization and increased char layer density. This suggests that SNC effectively promotes char formation and enhances the graphitization degree of the residual char, thereby reducing heat and oxygen transfer. These findings are consistent with the morphological features observed in the SEM images of the residual char.

The XPS spectra and elemental contents of EP and EP-SNC15 chars are presented in Fig. 6. Both EP and EP-SNC15 chars contain carbon, nitrogen, and oxygen. Additionally, selenium is also present in EP-SNC15 char, further confirming the condensed-phase flame-retardant effect of SNC (see Fig. 6b and Table S9). In detail, compared with EP char (5.15), the C/O atomic ratio of the EP-SNC15 char increases to 5.34, indicating that the introduction of SNC as a co-curing agent promotes the carbonization process and reduces the oxygen content in the residual char. The higher C/O ratio implies the formation of a denser and thermally stable char layer, which helps to inhibit heat transfer and the release of combustible materials during the combustion process, thus enhancing the overall flame retardant and smoke suppressant properties.

In addition, the high-resolution XPS C1s, N1s, and O1s spectra of EP-

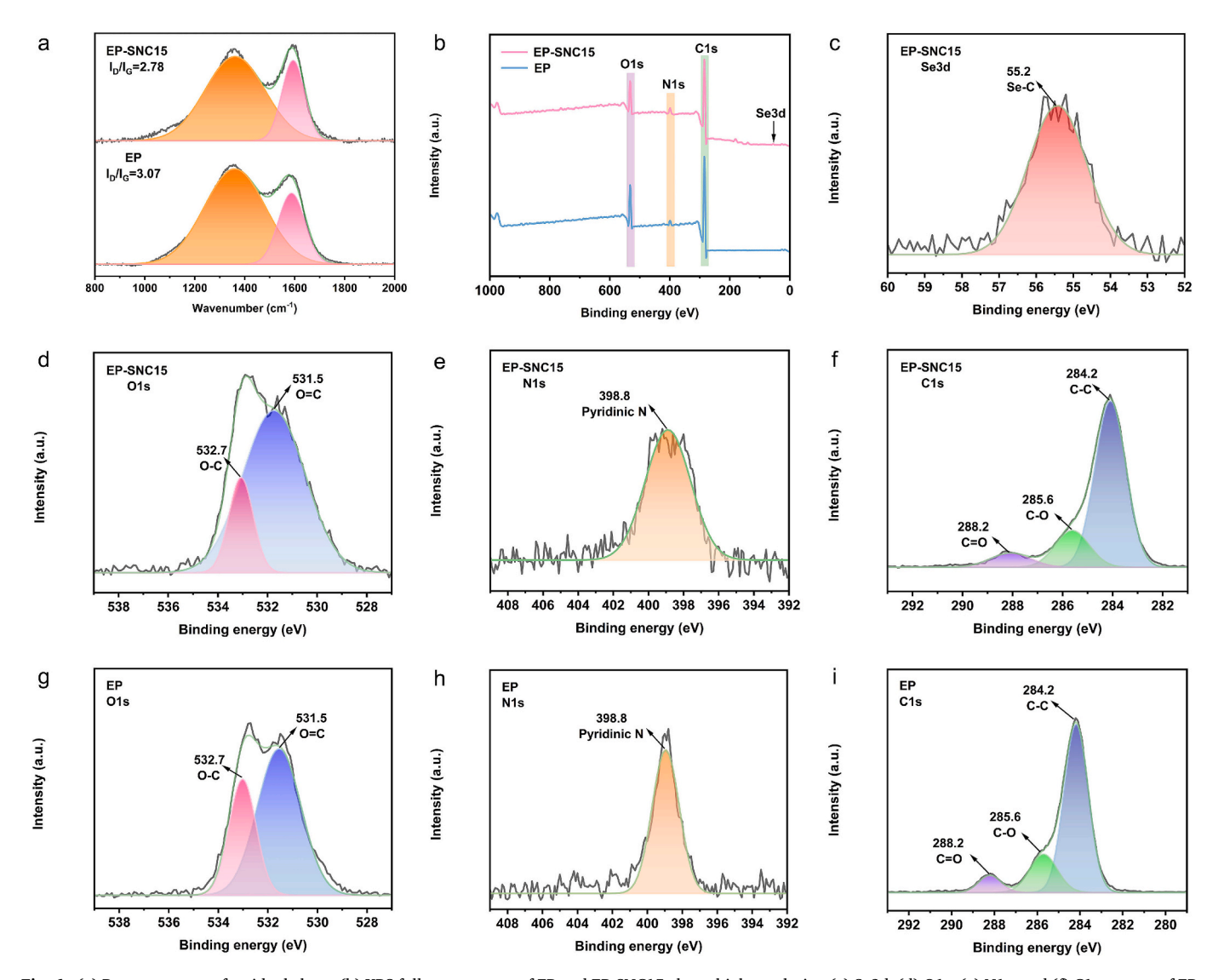


Fig. 6. (a) Raman spectra of residual chars; (b) XPS full-scan spectra of EP and EP-SNC15 chars; high-resolution (c) Se3d, (d) O1s, (e) N1s, and (f) C1s spectra of EP-SNC15 char; and high-resolution (g) O1s, (h) N1s, and (i) C1s spectra of EP char.

SNC15 char are similar to those of EP char (see Fig. 6d-i). Two deconvolution peaks at 532.7 and 531.5 eV are detected in the O1s spectra, corresponding to the O=C and O—C carbon oxide structures, respectively (Fig. 6d and g) [54]. The peak at 398.8 eV in the N1s spectra belongs to the pyridine-N- structure (Fig. 6e and h) [55]. The peaks at 284.2, 285.6 and 288.2 eV in the C1s spectra correspond to the C—C, C—O and C=O structures, respectively (Fig. 6f and i) [56]. Moreover, the high-resolution Se3d spectrum of EP-SNC15 char shows a characteristic peak of Se—C bonding at 55.2 eV, indicating that Se participates in the construction of stable char layers during the carbonization process (Fig. 6c) [13]. These results indicate that, during combustion, the catalytic carbonization effect of the Se-containing groups and Schiff base structures in EP-SNC15 enhances the graphitization degree of the residual char, protects the underlying matrix, and provides physical isolation, thereby contributing to its flame-retardant performance [57].

3.6.2. Gaseous phase

The mode action of SNC in the gas phase was analyzed *via* thermogravimetric infrared (TG-IR) and pyrolysis gas chromatography/mass spectrometry (Py-GC/MS) tests. As shown in Fig. 7a-c, EP and EP-SNC15 release similar decomposition products upon heating, including water (3724 cm⁻¹), hydrocarbons (2971 cm⁻¹), carbon dioxide (2360

cm⁻¹), carbonyl compounds (1713 cm⁻¹), aromatic compounds (1515 cm⁻¹ and 823 cm⁻¹), and ethers (1178 cm⁻¹) [41,42]. The peaks corresponding to ether derivatives, aromatic compounds, and hydrocarbons of the gaseous decomposition products for EP-SNC15 are lower than those for EP (see Fig. 7d-f), which further indicates that the degradation products of SNC inhibit pyrolysis by facilitating the carbonization of the substrate, thus protecting the substrate. Furthermore, the pyrolysis products of SNC were analyzed by Py-GC/MS, with the total ion chromatogram and major pyrolysis products shown in Fig. 7g and h. The main pyrolysis products of SNC are aliphatic amines, aromatic organic compounds and selenium-containing compounds. The N-containing derivatives released by SNC during combustion can dilute the concentration of flammable gases [58]. Furthermore, during the combustion process, the weak bond Se-N in SNC breaks to generate free radicals (Se·), which capture active free radicals from the EP matrix, thereby interrupting the chain reaction of combustion and thus inhibiting the combustion reaction [59].

The possible roles of SNC in the combustion process are shown in Fig. 8: (i) during pyrolysis, the Se- and N-containing fragments are released from the decomposition of SNC to dilute the concentration of combustible gases and trap the high-energy free radicals (\cdot OH and \cdot H) from epoxy matrix, thus inhibiting the combustion chain reaction in the

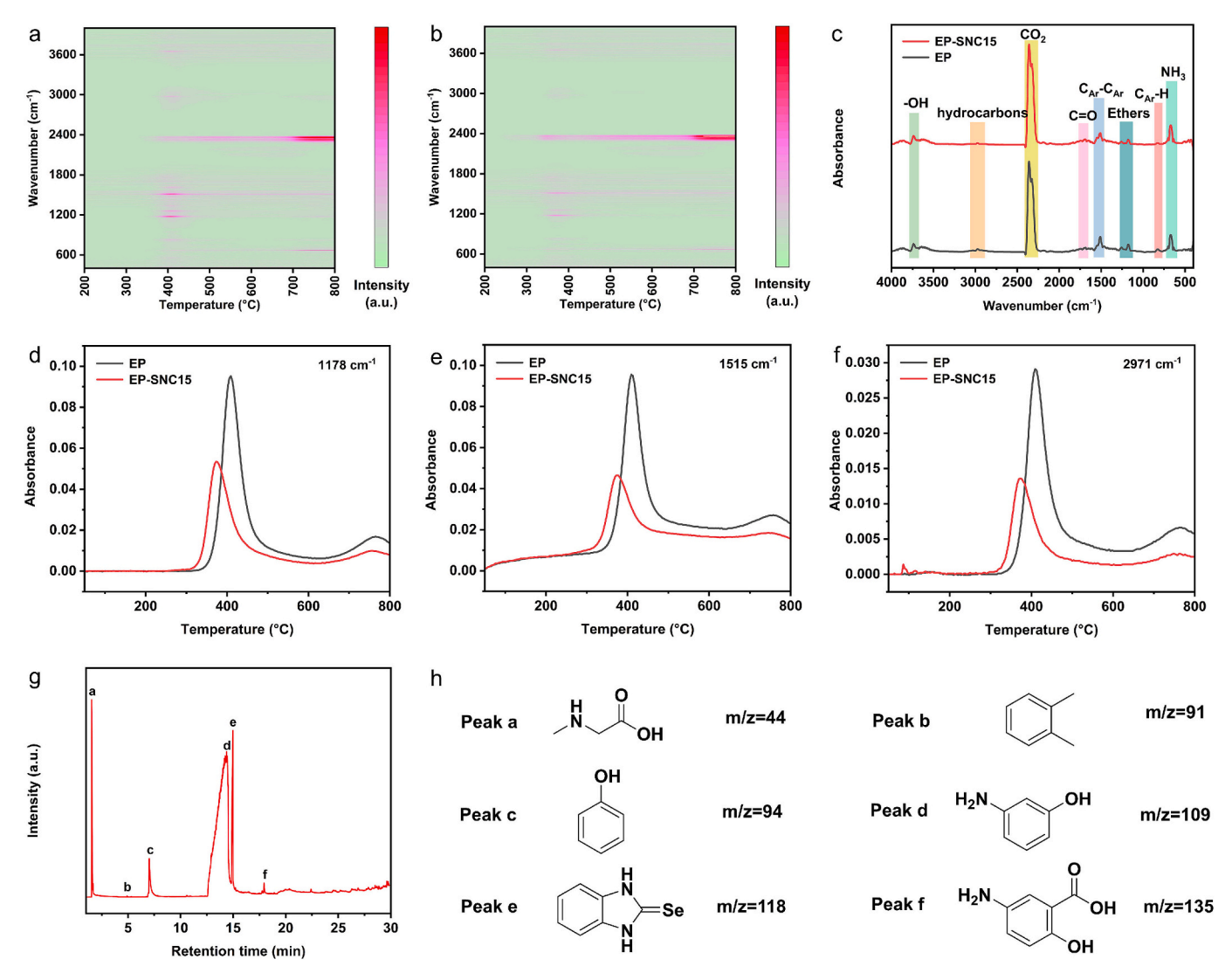


Fig. 7. TG-IR plots of the gaseous decomposition products of (a) EP and (b) EP-SNC15; (c) FTIR curves of EP and EP-SNC15 samples at temperature at maximum weight loss rate (T_{max}); absorbance and temperature curves of the gaseous decomposition products of EP and EP-SNC15 at (d) 1178, (e) 1515, and (f) 2971 cm⁻¹; (g) total ion chromatogram of SNC; and (h) pyrolysis products of SNC detected by Py-GC/MS.

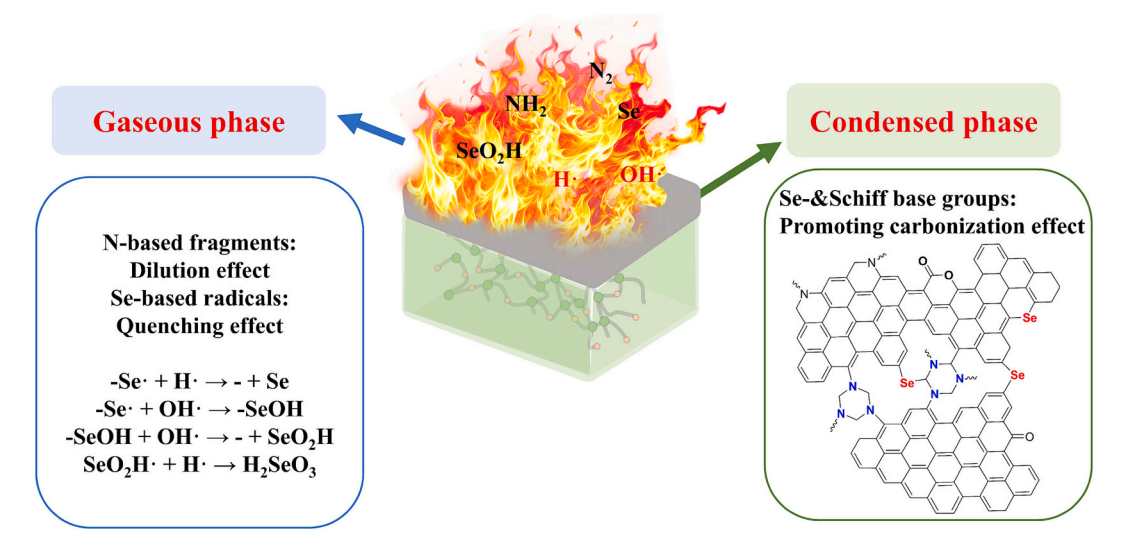


Fig. 8. The possible flame-retardant mechanism of SNC.

gas phase; (ii) In the condensed phase, the organic selenium group degrades into selenium-containing acids that catalyze the carbonization of the substrate, and the Schiff base groups enhance the densification and adiabatic properties of the char layer *via* their self-cross-linking reaction, thereby effectively hindering the transfer of heat and oxygen. Therefore, SNC acts in both the gas and condensed phases to suppress the heat release and smoke emission, thus improving fire safety of EP.

4. Conclusions

In this work, a selenium/Schiff base-containing bio-based co-curing agent was successfully synthesized using 3, 4-diaminotoluene, selenium dioxide and 5-aminosalicylic acid as raw materials and applied it to flame-retardant EPs. With the increase of SNC content, the flame retardancy and mechanical properties of EP-SNC significantly improve, and high thermal stability and good solvent resistance are effectively maintained. EP-SNC15 exhibits excellent mechanical robustness (tensile strength: 75.3 MPa) and flame-retardant performance (a UL-94 V-0 rating and an LOI of 31.8 %). Its PHRR and THR are reduced by 73.3 % and 56.3 %, respectively, compared to neat EP, outperforming previously reported phosphorus-free flame-retardant EPs. During combustion, the selenium-containing and Schiff-base groups in SNC promotes the formation of dense char layers, and the Se-containing fragments quench the active radicals in the gas phase, thereby suppressing combustion. This study provides a simple and effective approach for creating nextgeneration reactive flame retardants for epoxy systems, promoting the development of bio-based flame retardants.

CRediT authorship contribution statement

Qian Zhong: Writing – original draft, Visualization, Investigation. Cheng Wang: Writing – review & editing, Visualization. Guofeng Ye: Formal analysis. Zhenghong Guo: Investigation. Ting Sai: Formal analysis. Min Hong: Data curation. Pingan Song: Formal analysis. Hao Wang: Supervision. Siqi Huo: Writing – review & editing, Supervision, Project administration, Conceptualization. Zhitian Liu: Supervision, Project administration.

Declaration of competing interest

The authors declare that they have no known competing financial interests or personal relationships that could have appeared to influence the work reported in this paper.

Acknowledgements

This work was funded by the Australian Research Council (DE230100616), the Science Foundation of Wuhan Institute of Technology (24QD055), and the Foundation for 16th Graduate Education Innovation of Wuhan Institute of Technology (CX2024340).

Appendix A. Supplementary data

Supplementary data to this article can be found online at https://doi.org/10.1016/j.cej.2025.168756.

Data availability

Data will be made available on request.

References

- S. Huo, P. Song, B. Yu, S. Ran, V.S. Chevali, L. Liu, Z. Fang, H. Wang, Phosphoruscontaining flame retardant epoxy thermosets: Recent advances and future perspectives, Prog. Polym. Sci. 114 (2021) 101366, https://doi.org/10.1016/j. propolymsci 2021 101366
- [2] H. Wang, S. Huo, V. Chevali, W. Hall, A. Offringa, P. Song, H. Wang, Carbon Fiber Reinforced Thermoplastics: From Materials to Manufacturing and Applications, Adv. Mater. 37 (27) (2025) 2418709, https://doi.org/10.1002/adma.202418709.
- [3] Y. Guo, Q. Yang, S. Huo, J. Li, P. Jafari, Z. Fang, P. Song, H. Wang, Recyclable fire-retardant bio-based thermosets: From molecular engineering to performances and applications, Prog. Polym. Sci. 162 (2025) 101935, https://doi.org/10.1016/j.prognolymsci.2025.101935
- [4] G. Ye, S. Huo, C. Wang, Q. Zhang, B. Wang, Z. Guo, H. Wang, Z. Liu, Fabrication of flame-retardant, strong, and tough epoxy resins by solvent-free polymerization with bioderived, reactive flame retardant, Sustain. Mater. Technol. 39 (2024) e00853, https://doi.org/10.1016/j.susmat.2024.e00853.
- [5] P. Zheng, H. Zhao, Q. Liu, P/N synergistic integrated flame retardants with instant cross-linking at high-temperature for flame retardancy and impact resistance of epoxy resins, Polym. Degrad. Stab. 225 (2024) 110817, https://doi.org/10.1016/j. polymdegradstab. 2024.110817.
- [6] H. He, Q. Jiang, Y. Wan, M.H. Mia, X. Qu, M. Zhou, X. He, X. Li, M. Hong, Z. Yu, S. Huo, Biological skin-inspired damage warning and self-healing thermoelectric aerogel fiber via coaxial wet spinning for wearable temperature sensing, J. Mater. Sci. Technol. 250 (2025) 257–271, https://doi.org/10.1016/j.jmst.2025.06.038.
- [7] C. Wang, S. Huo, G. Ye, B. Wang, Z. Guo, Q. Zhang, P. Song, H. Wang, Z. Liu, Construction of an epoxidized, phosphorus-based poly(styrene butadiene styrene) and its application in high-performance epoxy resin, Compos. Part B 268 (2024) 111075, https://doi.org/10.1016/j.compositesb.2023.111075.
- [8] J. Wang, J. Wang, S. Yang, K. Chen, Single-component flame-retardant and smoke-suppressive epoxy resins enabled by an aluminum/phosphorus/imidazole-containing complex, Compos. Part B 253 (2023) 110571, https://doi.org/10.1016/j.compositesb.2023.110571.
- [9] Y. Chen, H. Duan, S. Ji, H. Ma, Novel phosphorus/nitrogen/boron-containing carboxylic acid as co-curing agent for fire safety of epoxy resin with enhanced

- mechanical properties, J. Hazard. Mater. 402 (2021) 123769, https://doi.org/10.1016/j.jhazmat.2020.123769.
- [10] R. Liu, Y. Zhang, W. Liu, Z. Yu, R. Yu, H. Yan, Hyperbranched Polyborophosphate towards Transparent Epoxy Resin with Ultrahigh Toughness and Fire Safety, Small 21 (24) (2025) 2502839, https://doi.org/10.1002/smll.202502839.
- [11] Y. Zhang, R. Liu, R. Yu, K. Yang, L. Guo, H. Yan, Phosphorus-free hyperbranched polyborate flame retardant: ultra-high strength and toughness, reduced fire hazards and unexpected transparency for epoxy resin, Compos. Part B 242 (2022) 110101, https://doi.org/10.1016/j.compositesb.2022.110101.
- [12] H. Niu, H. Nabipour, X. Wang, L. Song, Y. Hu, Phosphorus-Free Vanillin-Derived Intrinsically Flame-Retardant Epoxy Thermoset with Extremely Low Heat Release Rate and Smoke Emission, ACS Sustain. Chem. Eng. 9 (15) (2021) 5268–5277, https://doi.org/10.1021/acssuschemeng.0c08302.
- [13] X. Shang, Y. Jin, W. Du, L. Bai, R. Zhou, W. Zeng, K. Lin, Flame-Retardant and Self-Healing Waterborne Polyurethane Based on Organic Selenium, ACS Appl. Mater. Interfaces 15 (12) (2023) 16118–16131, https://doi.org/10.1021/ accami 3c02/251
- [14] X. Chen, S. Chen, Z. Xu, J. Zhang, M. Miao, D. Zhang, Degradable and recyclable bio-based thermoset epoxy resins, Green Chem. 22 (13) (2020) 4187–4198, https://doi.org/10.1039/d0gc01250e.
- [15] Y.J. Xu, K.T. Zhang, J.R. Wang, Y.Z. Wang, Biopolymer-based flame retardants and flame-retardant materials, Adv. Mater. (2025) 2414880, https://doi.org/10.1002/ adma.202414880.
- [16] C. Yan, Y.Q. Fang, R.F. Yang, M.F. Yan, W.H. Wang, Y.M. Song, Q.W. Wang, Preparation of amino wood coatings with superior flame retardancy, smoke suppression, and transparency using fully bio-based flame retardants, Polym. Degrad. Stab. 234 (2025) 111213, https://doi.org/10.1016/j. polymdegradstab.2025.111213.
- [17] Z.Q. Fan, Y.C. Li, J.T. He, B.Y. Song, M.Z. Chang, X.Y. Fang, L. Yu, G.C. Yang, H. W. Guo, Y. Liu, Bio-based intelligent multifunctional coating for wood: Flame retardancy, fire warning, smoke suppression, thermal insulation and antibacterial activity, Constr. Build. Mater. 465 (2025) 17, https://doi.org/10.1016/j.conbuildmat 2025 140244
- [18] X.F. Shi, F. Shi, C.Z. Luo, C.H. Zhang, L. Shang, Bio-based phosphorus multifunctional P/N flame retardant to improve synergistically the mechanical and fire resistance of epoxy resin, Mater. Today Chem. 46 (2025) 13, https://doi.org/ 10.1016/j.mtchem.2025.102755.
- [19] B.Y. Jiang, Y.X. Zhang, J. Gao, Y.T. Guo, J. Ying, G.H. Chen, J.H. Han, Y.M. Zhao, T.Y. Gao, Y.Z. Wang, Q. Wu, Y.M. Yu, S.N. Li, J.F. Dai, High-performance epoxy resin with flame-retardant, transparent, and ultraviolet shielding properties based on a vanillin-based multifunctional macromolecule, Int. J. Biol. Macromol. 277 (2024) 11, https://doi.org/10.1016/j.ijbiomac.2024.134275.
- [20] E.A. Agustiany, D.S. Nawawi, W. Fatriasari, M.U. Wahit, H. Vahabi, D.S. Kayla, L. S. Hua, Mechanical, morphological, thermal, and fire-retardant properties of sustainable chitosan-lignin based bioplastics, Int. J. Biol. Macromol. 306 (2025) 16. https://doi.org/10.1016/j.iibiomac.2025.141445.
- [21] X. Song, F. Song, X.-M. Ding, J.-M. Wu, X.-H. Wang, F. Wang, R. Feng, X.-L. Wang, Y.-Z. Wang, Construction of bio-based ramie fabric/epoxy resin composites with high flame retardant and mechanical performances, Ind. Crop. Prod. 194 (2023) 116281, https://doi.org/10.1016/j.indcrop.2023.116281.
- [22] W.X. Chen, H.B. Liu, Q.M. Yan, Q.H. Chen, M.C. Hong, Z.X. Zhou, H.Q. Fu, Straightforward synthesis of novel chitosan bio-based flame retardants and their application to epoxy resin flame retardancy, Composites, Communications 48 (2024) 1–14, https://doi.org/10.1016/j.coco.2024.101949.
- [23] J. Zhang, X. Mi, S. Chen, Z. Xu, D. Zhang, M. Miao, J. Wang, A bio-based hyperbranched flame retardant for epoxy resins, Chem. Eng. J. 381 (2020) 122719, https://doi.org/10.1016/j.cej.2019.122719.
- [24] X. Song, Z.-P. Deng, C.-B. Li, F. Song, X.-L. Wang, L. Chen, D.-M. Guo, Y.-Z. Wang, A bio-based epoxy resin derived from p-hydroxycinnamic acid with high mechanical properties and flame retardancy, Chin. Chem. Lett. 33 (11) (2022) 4912–4917, https://doi.org/10.1016/j.cclet.2021.12.067.
 [25] Y.X. Wang, X. Zheng, K.S. Jiang, D.Z. Han, Q.Q. Zhang, Bio-based melamine
- [25] Y.X. Wang, X. Zheng, K.S. Jiang, D.Z. Han, Q.Q. Zhang, Bio-based melamine formaldehyde resins for flame-retardant polyurethane foams, Int. J. Biol. Macromol. 273 (2024) 132836, https://doi.org/10.1016/j.ijbiomac.2024.132836.
- [26] S. Khodavandegar, P. Fatehi, Phytic acid derivatized lignin as a thermally stable and flame retardant material, Green Chem. 26 (19) (2024) 18, https://doi.org/ 10.1039/d4gc03169e.
- [27] W.F. Tang, X. Liao, Z.D. Qin, Y. Zeng, C. Chen, Q. Zhu, Z.H. Mo, X.D. Jin, Improving the flame retardancy of epoxy resin by incorporating a bio-based flame retardant and kaolinite, Polym. Degrad. Stab. 227 (2024) 110895, https://doi.org/ 10.1016/j.polymdegradstab.2024.110895.
- [28] J. Yu, C.C. Guo, J.K. Wang, J.X. Song, Y.P. Wang, J.J. Cheng, Y.F. Cheng, F. Zhang, Preparation of bio-based trinity lignin intumescent flame retardant and its effect on burning behavior and heat transfer process of epoxy resin composites, Prog. Org. Coat. 195 (2024) 108653, https://doi.org/10.1016/j.porgcoat.2024.108653.
- [29] S. Zhao, M.M. Abu-Omar, Recyclable and Malleable Epoxy Thermoset Bearing Aromatic Imine Bonds, Macromolecules 51 (23) (2018) 9816–9824, https://doi. org/10.1021/acs.macromol.8b01976.
- [30] J. Choi, K.H. Min, B.S. Kim, S.-H. Baeck, S.E. Shim, Y. Qian, Preparation of Ar-P-N-structured flame retardant via Kabachnik-Fields reaction for fire safety and mechanical reinforcement of polyurethane, Prog. Org. Coat. 186 (2024) 108081, https://doi.org/10.1016/j.porgcoat.2023.108081.
- [31] H.C.B. Paula, R.B.C. Silva, C.M. Santos, F.D.S. Dantas, R.C.M. de Paula, L.R.M. de Lima, E.F. de Oliveira, E.A.T. Figueiredo, F.G.B. Dias, Eco-friendly synthesis of an alkyl chitosan derivative, Int. J. Biol. Macromol. 163 (2020) 1591–1598, https:// doi.org/10.1016/j.ijbiomac.2020.08.058.

- [32] Q. Chen, J. Feng, Y. Xue, S. Huo, T. Dinh, H. Xu, Y. Shi, J. Gao, L.-C. Tang, G. Huang, W. Lei, P. Song, An Engineered Heterostructured Trinity Enables Fire-Safe, Thermally Conductive Polymer Nanocomposite Films with Low Dielectric Loss, Nano-Micro Letters 17 (1) (2025) 168, https://doi.org/10.1007/s40820-025-01681-0
- [33] Y. Yi, H. Xu, L. Wang, W. Cao, X. Zhang, A New Dynamic Covalent Bond of Se-N: Towards Controlled Self-Assembly and Disassembly, Chem.—Eur. J. 19 (29) (2013) 9506–9510, https://doi.org/10.1002/chem.201301446.
- [34] Z. Zhang, J. Qin, W. Zhang, Y.-T. Pan, D.-Y. Wang, R. Yang, Synthesis of a novel dual layered double hydroxide hybrid nanomaterial and its application in epoxy nanocomposites, Chem. Eng. J. 381 (2020) 122777, https://doi.org/10.1016/j. cei.2019.122777.
- [35] A.H. Bui, A.D. Fernando Pulle, A.S. Micallef, J.J. Lessard, B.T. Tuten, Dynamic chalcogen squares for material and topological control over macromolecules, Angew. Chem. Int. Ed. 63 (22) (2024) 1–5, https://doi.org/10.1002/ apie 202404474
- [36] G. Ye, S. Huo, C. Wang, P. Song, Z. Fang, H. Wang, Z. Liu, Durable flame-retardant, strong and tough epoxy resins with well-preserved thermal and optical properties via introducing a bio-based, phosphorus-phosphorus, hyperbranched oligomer, Polym. Degrad. Stab. 207 (2023) 110235, https://doi.org/10.1016/j. polymdegradstab. 2022.110235.
- [37] Y.-F. Xiao, S. Gu, F.-M. He, Y. Wang, C. Liu, Y.-Z. Wang, L. Chen, Towards superb toughness, strength, and flame retardancy in epoxy resins via molecular interface engineering, Compos. Part B 297 (2025) 112293, https://doi.org/10.1016/j.compositesb.2025.112293.
- [38] H. Li, C. Liu, J. Zhu, X. Huan, K. Xu, H. Geng, X. Chen, T. Li, D. Deng, W. Ding, L. Zu, L. Ge, X. Jia, X. Yang, Intrinsically reactive hyperbranched interface governs graphene oxide dispersion and crosslinking in epoxy for enhanced flame retardancy, J. Colloid Interface Sci. 672 (2024) 465–476, https://doi.org/10.1016/ ijcis.2024.06.005.
- [39] X.-F. Liu, Y.-F. Xiao, X. Luo, B.-W. Liu, D.-M. Guo, L. Chen, Y.-Z. Wang, Flame-Retardant multifunctional epoxy resin with high performances, Chem. Eng. J. 427 (2022) 2145, https://doi.org/10.1016/j.cej.2021.132031.
- [40] G. Wang, Q. He, K. Niu, One-step solution self-assembly synthesis of biomass-based flame retardants for constructing epoxy resins with superior flame retardant properties, Constr. Build. Mater. 483 (2025) 141706, https://doi.org/10.1016/j. conbuildmat.2025.141706.
- [41] C. Wang, G. Ye, Q. Zhang, H. Wang, S. Huo, Z. Liu, Closed-Loop Recyclable, Self-Catalytic Transesterification Vitrimer Coatings with Superior Adhesive Strength, Fire Retardancy, and Environmental Stability, ACS Mater. Lett. 7 (1) (2024) 210–219, https://doi.org/10.1021/acsmaterialslett.4c02235.
- [42] G. Ye, S. Huo, C. Wang, Q. Zhang, H. Wang, P. Song, Z. Liu, Strong yet tough catalyst-free transesterification vitrimer with excellent fire-retardancy, durability, and closed-loop recyclability, Small 20 (45) (2024) 2404634, https://doi.org/ 10.1002/smll.202404634.
- [43] Y. Lv, J. Dai, L. Xia, L. Luo, Y. Xu, L. Dai, Smoke suppression and phosphorus-free condensed phase flame-retardant epoxy resin composites based on Salen-Ni, Polym. Degrad. Stab. 201 (2022) 109980, https://doi.org/10.1016/j. polymdegradstab. 2022.109980.
- [44] R. Wang, P. Zheng, J. Li, J. Sun, H. Liu, X. Li, Q. Liu, An Efficient Cross-Linked Phosphorus-Free Flame Retardant for Epoxy Resins, ACS Omega 7 (42) (2022) 37170–37179. https://doi.org/10.1021/acsomega.2c03167.
- [45] X. Ye, W. Zhang, R. Yang, J. He, J. Li, F. Zhao, Facile synthesis of lithium containing polyhedral oligomeric phenyl silsesquioxane and its superior performance in transparency, smoke suppression and flame retardancy of epoxy resin, Compos. Sci. Technol. 189 (2020) 108004, https://doi.org/10.1016/j. compscitech.2020.108004.
- [46] P. Zheng, R. Wang, X. Peng, J. Sun, H. Liu, J. Li, C. Liu, L. Jiang, Q. Liu, Y. Zhang, Halogen-free and phosphorus-free flame retardants endow epoxy resin with high flame retardancy through crosslinking strategy, High Perform. Polym. 34 (5) (2022) 560–567, https://doi.org/10.1177/09540083221085170.
- (2022) 560–567, https://doi.org/10.1177/09540083221085170.
 [47] H. Ou, J. Li, M. Jin, J. Ren, Eugenol-derived trifunctional epoxy resin: Intrinsic phosphorus-free flame retardancy and mechanical reinforcement for sustainable polymer alternatives, Polym. Degrad. Stab. 239 (2025) 111394, https://doi.org/10.1016/j.polymdegradstab. 2025.111394.
- [48] S. Wang, F. Sun, Z. Ni, Y. Lyu, T. Kaneko, W. Dong, M. Chen, D. Shi, Aromatic Epoxy from Caffeic Acid: Mechanical Properties and Flame Retardancy, ACS Sustain. Chem. Eng. 12 (29) (2024) 10713–10726, https://doi.org/10.1021/ acssschemeng.4c01107
- [49] X.-H. Shi, H. Shi, X.-L. Li, S.-J. Wu, W.-M. Xie, D.-Y. Wang, Polydopamine-primed FeCo-LDH endowed epoxy resin with enhanced flame retardancy and mechanical properties, Constr. Build. Mater. 439 (2024) 137070, https://doi.org/10.1016/j. arxivillar.ex/2024.137070
- [50] Y.-m.-z. Zhang, M.-y. Huang, J. Zhou, D.-z. Li, Y. Lei, Synthesis and characterization of a chalcone-derived epoxy containing pyrazoline ring with excellent flame resistance, High Perform. Polym. 33 (7) (2021) 785–796, https://doi.org/10.1177/0954008321993523.
- [51] S. Zhang, Y. Jiang, Y. Sun, J. Sun, B. Xu, H. Li, X. Gu, Preparation of flame retardant and conductive epoxy resin composites by incorporating functionalized multi-walled carbon nanotubes and graphite sheets, Polym. Adv. Technol. 32 (5) (2021) 2093–2101, https://doi.org/10.1002/pat.5239.
- [52] Y. Cui, Y. Jiao, G. Zhang, Z. Huo, J. Sun, H. Qu, J. Xu, Biomass-derived polyelectrolyte fire retardant: synergistic phosphorus-nitrogen doping for enhanced epoxy resin flame retardancy and smoke suppression, Polym. Degrad. Stab. 234 (2025) 111207, https://doi.org/10.1016/j. polymdegradstab.2025.111207.

- [53] Z. Ma, J. Feng, S. Huo, Z. Sun, S. Bourbigot, H. Wang, J. Gao, L.C. Tang, W. Zheng, P. Song, Mussel-Inspired, Self-Healing, Highly Effective Fully Polymeric Fire-Retardant Coatings Enabled by Group Synergy, Adv. Mater. 36 (44) (2024) 2410453, https://doi.org/10.1002/adma.202410453.
 [54] G. Ye, S. Huo, C. Wang, Y. Guo, Q. Yang, P. Song, H. Wang, Z. Liu, A transparent
- [54] G. Ye, S. Huo, C. Wang, Y. Guo, Q. Yang, P. Song, H. Wang, Z. Liu, A transparent epoxy vitrimer with outstanding flame retardancy, toughness, and recyclability enabled by a hyperbranched P/N-derived polyester, Constr. Build. Mater. 470 (2025) 140673, https://doi.org/10.1016/j.conbuildmat.2025.140673.
- [55] S. Huo, Z. Zhou, J. Jiang, T. Sai, S. Ran, Z. Fang, P. Song, H. Wang, Flame-retardant, transparent, mechanically-strong and tough epoxy resin enabled by high-efficiency multifunctional boron-based polyphosphonamide, Chem. Eng. J. 427 (2022) 131578, https://doi.org/10.1016/j.cej.2021.131578.
- [56] H. Wang, Y. Wang, J. Gao, Z. Zhu, F. Xiao, Synergistic engineering of phosphaphenanthrene and ionic liquids for unlocking flame retardant

- multifunctional epoxy resin with high performances, Polym. Degrad. Stab. 239 (2025) 111407, https://doi.org/10.1016/j.polymdegradstab. 2025.111407.
- [57] T. Sai, X. Ye, B. Wang, Z. Guo, J. Li, Z. Fang, S. Huo, Transparent, intrinsically fire-safe yet impact-resistant poly(carbonates-b-siloxanes) containing Schiff-base and naphthalene-sulfonate, J. Mater. Sci. Technol. 225 (2025) 11–20, https://doi.org/10.1016/j.jmst.2024.11.023.
- [58] C. Wang, S. Huo, G. Ye, Q. Zhang, C.-F. Cao, M. Lynch, H. Wang, P. Song, Z. Liu, Strong self-healing close-loop recyclable vitrimers via complementary dynamic covalent/non-covalent bonding, Chem. Eng. J. 500 (2024) 157418, https://doi. org/10.1016/j.cej.2024.157418.
- [59] F. Wei, Y. Wu, M. Li, D. Pei, C. Li, Hydrogen bond cross-linked photo-healable multifunctional phase change materials for thermal management, J Energy Storage 106 (2025) 114821, https://doi.org/10.1016/j.est.2024.114821.